In vivo relationship between joint stiffness, joint-based estimates of muscle stiffness, and shear-wave velocity

Andrew D. Vigotsky, *Student Member, IEEE*, Elliott J. Rouse, *Member, IEEE,* and Sabrina S.M. Lee

***Abstract*— Shear-wave (SW) ultrasound elastography is both a clinical and research tool that is increasingly being used to quantify the material properties of muscle. However, how SW velocity relates to stiffness changes on the joint- and muscle-levels is poorly understood. Therefore, the purpose of this work was to develop a biomechanical model to estimate plantar flexor muscle stiffness, and measure joint stiffness, joint-based estimates of muscle stiffness, and medial gastrocnemius (MG) SW velocity under different activations (0, 20, and 40%) to quantify the relationships between 1) joint stiffness and joint-based estimates of muscle stiffness; 2) joint stiffness and MG SW velocity; and 3) joint-based estimates of muscle stiffness and MG SW velocity. Our main findings include strong relationships between 1) joint stiffness and joint-based estimates of muscle stiffness ($R^2 = 0.70$) and 2) joint stiffness and MG SW velocity ($R^2 = 0.66$), and a weak relationship between joint-based estimates of muscle stiffness and MG SW velocity ($R^2 = 0.24$). These findings further our understanding of SW velocity measures in muscle and provide a biomechanical model to decompose muscle stiffness from joint stiffness.**

I. Introduction

The biomechanical properties of a joint are mediated by the surrounding tissues, all of which have individual contributions that cannot be distinguished on the joint level. Joint stiffness, which governs how a joint interacts with the environment and responds to external perturbations, is often studied at the joint level [1]. Researchers frequently take a heuristic approach to assessing the properties of the tissues that regulate joint stiffness, in that measurements are made on the joint level and it is assumed that they are representative of the state of the underlying tissue(s) of interest. These measures of joint stiffness have been investigated in a number of ways. Most commonly, the derivative of the net joint moment (M_{net}) with respect to joint angle (θ) ($\frac{dM_{net}}{d\theta}$) is calculated [2], [3]. Alternatively, perturbations can be applied to the joint to separate joint stiffness from damping and inertial components [1], [2], [4], [5]. While these descriptions provide useful information as to how the joint functions as a whole, they lack the specificity that may be needed to understand changes in joint stiffness and function. It remains unclear how gross measures of joint stiffness relate to the properties of the tissues surrounding that joint.

Research supported by the American Society of Biomechanics' Graduate Student Grant-In-Aid. This material is based upon work supported by the National Science Foundation Graduate Research Fellowship under Grant No. DGE-1324585.

A. D. Vigotsky is with the Department of Biomedical Engineering, Northwestern University, Evanston, IL 60201 USA.

E. J. Rouse is with the Neurobionics Lab & Department of Mechanical Engineering, University of Michigan, Ann Arbor, MI 48109 USA

S. S. Lee is with the Department of Physical Therapy and Human Movement Sciences, Northwestern University, Chicago, IL, 60611 USA

Shear-wave (SW) ultrasound elastography is a promising method to measure the material properties of tissues. Shear-wave ultrasound elastography harnesses the same acoustic radiation forces as standard B-mode ultrasound; multiple ultrasound push beams are emitted to induce SWs, from which SW velocity can be measured; these SWs travel faster in stiffer tissues [6]. Shear-wave elastography has been used to characterize changes in muscle properties as a function of position [7], [8] and activation [8]. However, the relationship between SW velocity and joint stiffness is less understood. Previous investigations have not found a strong association between SW measures and joint stiffness, measured using the slope of the net joint moment-angle relationship [9], [10]. The net joint moment-angle relationship is limited in that 1) it is not related of short-range stiffness, which is the stiffness of muscle due to cross-bridging that is observed with small excursions [1], [11], and 2) is subject to multiple sources of resistance, such as damping and inertia [2]. Moreover, the relationship between *in vivo* joint-based estimates of muscle stiffness—which necessitates a modeling approach—and SW measures has not yet been explored. Thus, more rigorous investigation, combined with modeling, is needed to elucidate the relationship between SW velocity, more sophisticated measures of joint stiffness, and joint-based estimates of muscle stiffness (herein referred to as *estimates of muscle stiffness*).

The purpose of this experiment was to investigate the relationships between SW velocity, joint stiffness, and estimates of muscle stiffness. By understanding how SW velocity may or may not be related to joint and muscle stiffness, practitioners and researchers can better interpret, and thus apply, SW velocity data. It was hypothesized that linear relationships would be observed between 1) joint stiffness and estimates of muscle stiffness; 2) joint stiffness and SW velocity; and 3) estimates of muscle stiffness and SW velocity.

II. Methods

A. Participants

Four healthy young adults (age = 26 ± 6 years; height = 169.4 ± 9.7 cm; mass = 67.7 ± 17.8 kg) were recruited to participate in this study. All participants did not have any lower extremity musculoskeletal or neuromuscular pathology or pain for at least one year prior to participation and provided informed consent before beginning. This study was approved by the Northwestern University Institutional Review Board.

978-1-5386-3646-6/18/$31.00 ©2018 IEEE

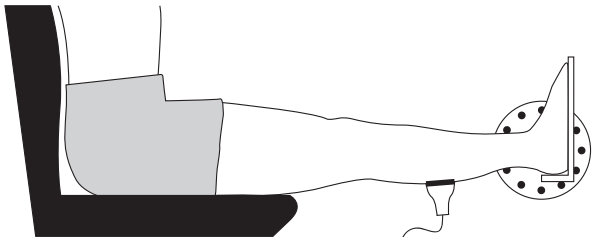

Fig. 1. Experimental setup. Each participant sat with their hips flexed 85°, ipsilateral knee fully extended, and ipsilateral ankle positioned to 90°.

B. Experimental Setup

Each participant sat in the Neurobionics Rotary Dynamometer—a custom frame-mounted motor (model: BSM90N-3150AF, Baldor, Fort Smith, AR, USA) with a six-axis load cell (model: 45E15A4, JR3, Inc., Woodland, CA, USA) coupled to an adjustable chair (model: 835-000, Biodex Medical Systems, Shirley, NY, USA) [12]—with their hips flexed 85°, ipsilateral (right) knee in full extension, and ipsilateral (right) ankle at 90°, with the sagittal plane ankle axis of rotation collinear with that of the motor (Figure 1). Sagittal plane, filtered Gaussian white noise perturbations with a mean amplitude of 1° and a cutoff frequency of 5 Hz were applied to each participant's ankle. Small amplitudes and low frequencies better represent short-range stiffness and limit reflex contributions, respectively [1]. During SW trials, the same setup was used, but no perturbations were applied. All kinetic and kinematic data were sampled at 2500 Hz. Kinetic data from SW trials were low-pass filtered with a zero-lag sixth-order Butterworth filter with a 5 Hz cutoff frequency and smoothed with a trailing average of 1000 ms to account for the delay in SW imaging.

Ultrasound images were obtained from the medial gastrocnemius (MG) muscle-tendon junction (B-mode only) and the muscle bellies of the MG, soleus, and tibialis anterior (B-mode and SW) (Aixplorer SuperSonic Imagine, Aix en Provence, France). A 1 cm × 1 cm region of interest was used to obtain estimates of SW velocity; this region was then trimmed to exclude anatomical structures other than the muscle belly of interest (*e.g.*, aponeuroses, other muscles). Shear-wave velocities within the cropped region of interest were averaged for each trial. The mean SW velocity for each muscle at each activation was then calculated for each participant.

C. Protocol

Plantar and dorsiflexion maximum voluntary contractions (MVC) were collected over three, five-second trials for each direction. Achilles' stiffness was estimated by imaging the MG muscle-tendon junction displacements during ramp isometric plantar flexion contractions (0–60% MVC). Finally, SW and perturbation trials were collected. Shear-wave images were recorded from different muscles in a randomized fashion, at three activations per muscle (0, 20, and 40% MVC, randomized). A total of six SW images were taken for each activation for each muscle. Perturbation trials were collected in a randomized order between SW trials, for a total of 27 trials per activation. Twenty-seven trials was chosen to keep the 95% confidence interval (CI) of the stiffness estimates for a given activation to be less than ±10% of the mean stiffness estimate for that activation (*i.e.*, $\frac{95\%\text{CI}}{\bar{x}} < 0.10$).

D. Joint and Muscle Stiffness

Data collected during the perturbation trials were analyzed using a system identification method described previously [13]. Briefly, using all trials for a given activation, an impedance impulse-response function (IRF) was estimated from the pseudoinverse of the auto-correlation matrix (ϕ_{xx}) and an averaged time-varying and time-invariant cross-correlation (ϕ_{xy}). The time-varying portion of the algorithm was used to account for any changes in strategy, which was evidenced by non-zero moments out of plane. The impedance IRFs were numerically integrated to obtain joint stiffness estimates. Each participant's 27 trials were analyzed together, such that the system identification algorithm would produce one estimate.

A biomechanical model was used to estimate muscle stiffness (k_m). First, moment arms ($r = {}^{dl}/_{d\theta}$) for the passive trials were estimated using MG moment arms from OpenSim (Stanford, CA, USA) [14], [15]. To account for increases in moment arm during activation due to bulging, moment arm values for active trials were multiplied by 1.185 [16]. Second, using each participant's moment arm estimate, tendon force ($F = {}^{M_{net}}/_{r}$) was calculated from ramp contraction trials. During these trials, each participant performed a slow, ramp isometric contraction, from 0 to 60% MVC, while the displacement of the MG muscle-tendon junction was tracked with B-mode ultrasound. Tendon forces and the associated tendon elongations (*i.e.*, muscle-tendon junction displacement) were then used to estimate tendon compliance ($k_t^{-1} = {}^{dl}/_{dF}$). Finally, the muscle was modeled to be in series with the tendon, which acts about the joint center from a distance, its moment arm, ${}^{dl}/_{d\theta}$. Thus, a net joint moment can be defined as

$$M_{net} = \left(k_t^{-1} + k_m^{-1}\right)^{-1} (\Delta l)\, \frac{dl}{d\theta}, \tag{1}$$

where Δl is the MTU's theoretical excursion from 'resting length'. It follows that, mechanically, the derivative of M_{net} with respect to the joint angle is joint stiffness

$$\frac{dM_{net}}{d\theta} = \left(k_t^{-1} + k_m^{-1}\right)^{-1} \left[\frac{d^2 l}{d\theta^2}\Delta l + \left(\frac{dl}{d\theta}\right)^2\right], \tag{2}$$

from which k_m could be estimated.

E. Statistical Analysis

To investigate the hypotheses that linear relationships exist between 1) joint stiffness and estimates of muscle stiffness; 2) joint stiffness and SW velocity; and 3) estimates of muscle stiffness and SW velocity, statistical analyses were carried out in R (version 3.4.2) [17]. After assumptions were ensured [18], bivariate linear regressions were performed to assess

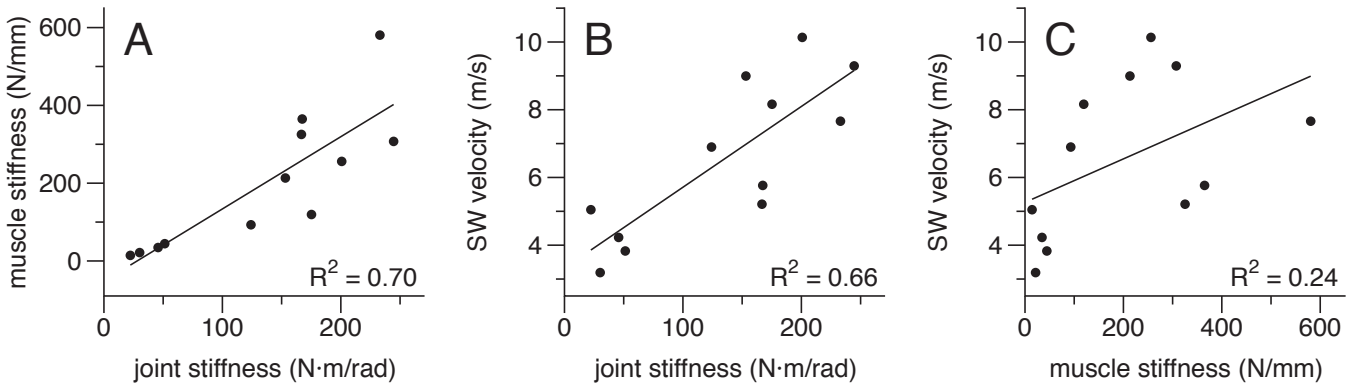

Fig. 2. Relationships between joint stiffness, estimates of muscle stiffness, and shear-wave velocity.

the aforementioned relationships. To avoid dichotomization of the interpretation of evidence, no *a priori* α-level was defined; rather, evidence for a relationship was interpreted on a continuum, using a combination of effect-sizes (R^2), CIs [19], *p*-values, Bayes factors (BF_{10}) [20], and theory [21].

III. Results

Strong linear relationships were observed between joint stiffness and MG SW velocity ($F_{1,10} = 19.59$; $p = 0.0013$; $R^2 = 0.662$ [$CI_{95} = 0.429$–0.895]; $BF_{10} = 44.15$) and joint stiffness and estimates of muscle stiffness ($F_{1,10} = 23.40$; $p = 0.0007$; $R^2 = 0.701$ [$CI_{95} = 0.488$–0.913]; $BF_{10} = 37.80$) (Figures 2A and 2B). However, only a weak relationship was observed between estimates of muscle stiffness and MG SW velocity ($F_{1,10} = 3.09$; $p = 0.1094$; $R^2 = 0.236$ [$CI_{95} = -0.078$–0.550]; $BF_{10} = 1.14$) (Figure 2C).

IV. Discussion

This study assessed the relationships between SW velocity, joint stiffness, and estimates of muscle stiffness. In agreement with hypotheses 1 and 2, strong relationships were observed between joint stiffness and estimates of muscle stiffness, and joint stiffness and MG SW velocity. However, unexpectedly, the relationship observed between estimates of muscle stiffness and MG SW velocity was weak (Figure 2C). These results have important implications for interpreting SW velocity.

Shear-wave velocity, muscle stiffness, and joint stiffness assess related constructs on different levels. Shear-wave velocity measures the local properties of the tissue(s) through which the SWs propagate, whereas muscle stiffness is indicative of the biomechanical properties of the muscle as whole. The stiffness of a muscle interacts with the length-dependent stiffness of its tendon [22]. During active conditions, muscle force lengthens the tendon, which increases k_t. The equivalent stiffness of the muscle and tendon in series is muscle-tendon unit (MTU) stiffness, which acts about a joint from a distance to contribute to joint stiffness (Figure 2A). Therefore, while muscle stiffness is related to joint stiffness, the relationship is not perfectly linear. Despite this, linear relationships were observed between joint stiffness and both SW velocity and estimates of muscle stiffness (Figures 2A–B). Under passive conditions, shear modulus, which is proportional to the square of SW velocity, is linearly related to Young's modulus as assessed using tensile testing [23]. Because the Young's moduli reported by Eby *et al*. [23] assume a constant cross-sectional area, the square of the SW velocity is necessarily related to muscle stiffness within a given muscle. Notwithstanding the findings of Eby *et al*. [23], no strong relationship was found between SW velocity and estimates of muscle stiffness in this present investigation (Figure 2C). Whether this null finding is a product of model limitations or some other factor necessitates further investigation, especially because a strong relationship was observed between SW velocity and joint stiffness (Figure 2B).

Joint stiffness is composed of more than a single MTU; other MTUs, fascia, ligaments, capsules, and friction will also contribute. Contributions from passive elements that act in parallel to the MTU, such as the joint capsule, will remain constant for all activations and will not affect the slope of the modeled relationship (Figure 2C). Conversely, stiffness contributions from muscles and series elastic elements will be force-dependent (Figure 2A). At greater activations, when $k_m \gg k_t$, the role of tendon stiffness increases, because MTU stiffness can only be as great as its most compliant element; this partially explains the slight heteroscedasticity in Figure 2A. The predictive relationship between muscle stiffness and joint stiffness has been previously explicated in the upper extremities [24], and this present work confirms that this relationship also holds in the ankle joint.

The plantar flexors are composed of multiple muscles, all of which may have unique contributions to joint stiffness. Despite the strong relationship between muscle stiffness and joint stiffness observed in this study (Figure 2A), the modeled muscle stiffness may not truly be indicative of MG muscle stiffness. Medial gastrocnemius has a relatively small contribution to the total physiological cross-sectional area, and thus, force-generating potential, of the triceps surae [25]. Furthermore, subject-specific k_t was estimated using the

displacement of the MG subtendon and the estimated force of the entire triceps surae; however, because each subtendon has a different stiffness [26], our k_t is likely indicative of a crude, rather than actual, estimate of tendon stiffness. Future work may model discrete muscles and their respective subtendons, as has been done for the upper extremity [24], while also accounting for differences in architecture. Such work may reveal a stronger relationship between MG SW velocity and muscle stiffness.

The observed relationships provide a foundation for interpreting joint stiffness, muscle stiffness, and SW velocity. Joint stiffness determines how a joint interacts with its environment and, therefore, may be most relevant for function. However, the specificity provided by muscle stiffness and SW velocity can provide useful insight; *e.g.*, when seeking to understand the etiology of changes joint stiffness. In contrast to previous work [9], [10], we have shown that changes in SW velocity are reflected on the joint level (Figure 2B), and therefore may be useful for understanding muscular origins of joint stiffness.

A. Limitations

There are a number of limitations concerning this study and the biomechanical model. While previous work has found that stiffness models are most sensitive to moment arms [24], the extent to which our model is sensitive is noteworthy; if OpenSim moment arms were not increased for the active state, up to 40-fold increases in muscle stiffness are observed. These differences likely arise from model complexity and type. Hu *et al*. [24] incorporated several MTUs to predict endpoint stiffness, whereas we back-calculated muscle stiffness, with the assumption that only a single MTU contributed to joint stiffness. Finally, our statistical model represents a between-subject relationship and may be confounded by individual differences. However, between-subject modeling allows for between-individual generalizations, which may be applicable for between-subject studies and clinical uses of SW ultrasound.

V. Acknowledgements

The authors would like to thank Dr. Daniel Ludvig for his technical assistance.

References

[1] R. E. Kearney and I. W. Hunter, "System identification of human joint dynamics." *Critical reviews in biomedical engineering*, vol. 18, no. 1, pp. 55–87, 1990.

[2] M. L. Latash and V. M. Zatsiorsky, "Joint stiffness: Myth or reality?" *Human movement science*, vol. 12, no. 6, pp. 653–692, 1993.

[3] E. J. Rouse, R. D. Gregg, L. J. Hargrove, and J. W. Sensinger, "The difference between stiffness and quasi-stiffness in the context of biomechanical modeling," *IEEE Transactions on Biomedical Engineering*, vol. 60, no. 2, pp. 562–568, 2013.

[4] E. J. Rouse, L. J. Hargrove, E. J. Perreault, and T. A. Kuiken, "Estimation of human ankle impedance during the stance phase of walking," *IEEE Transactions on Neural Systems and Rehabilitation Engineering*, vol. 22, no. 4, pp. 870–878, 2014.

[5] A. L. Shorter and E. J. Rouse, "Mechanical impedance of the ankle during the terminal stance phase of walking," *IEEE Transactions on Neural Systems and Rehabilitation Engineering*, 2017.

[6] J. Bercoff, M. Tanter, and M. Fink, "Supersonic shear imaging: a new technique for soft tissue elasticity mapping," *IEEE transactions on ultrasonics, ferroelectrics, and frequency control*, vol. 51, no. 4, pp. 396–409, 2004.

[7] G. Le Sant, A. Nordez, R. Andrade, F. Hug, S. Freitas, and R. Gross, "Stiffness mapping of lower leg muscles during passive dorsiflexion," *Journal of Anatomy*, vol. 230, no. 5, pp. 639–650, 2017.

[8] L. Chernak, R. DeWall, K. Lee, and D. Thelen, "Length and activation dependent variations in muscle shear wave speed," *Physiological measurement*, vol. 34, no. 6, p. 713, 2013.

[9] K. Chino and H. Takahashi, "The association of muscle and tendon elasticity with passive joint stiffness: in vivo measurements using ultrasound shear wave elastography," *Clinical Biomechanics*, vol. 30, no. 10, pp. 1230–1235, 2015.

[10] ——, "Measurement of gastrocnemius muscle elasticity by shear wave elastography: association with passive ankle joint stiffness and sex differences," *European journal of applied physiology*, vol. 116, no. 4, pp. 823–830, 2016.

[11] P. M. Rack and D. Westbury, "The short range stiffness of active mammalian muscle and its effect on mechanical properties," *The Journal of physiology*, vol. 240, no. 2, pp. 331–350, 1974.

[12] A. F. Azocar and E. J. Rouse, "Stiffness perception during active ankle and knee movement," *IEEE Trans Biomed Eng*, 2017.

[13] D. Ludvig and E. J. Perreault, "System identification of physiological systems using short data segments," *IEEE Transactions on Biomedical Engineering*, vol. 59, no. 12, pp. 3541–3549, 2012.

[14] E. M. Arnold, S. R. Ward, R. L. Lieber, and S. L. Delp, "A model of the lower limb for analysis of human movement," *Annals of biomedical engineering*, vol. 38, no. 2, pp. 269–279, 2010.

[15] S. L. Delp, F. C. Anderson, A. S. Arnold, P. Loan, A. Habib, C. T. John, E. Guendelman, and D. G. Thelen, "Opensim: open-source software to create and analyze dynamic simulations of movement," *IEEE transactions on biomedical engineering*, vol. 54, no. 11, pp. 1940–1950, 2007.

[16] S. Hashizume, S. Iwanuma, R. Akagi, H. Kanehisa, Y. Kawakami, and T. Yanai, "The contraction-induced increase in achilles tendon moment arm: A three-dimensional study," *Journal of biomechanics*, vol. 47, no. 12, pp. 3226–3231, 2014.

[17] R Core Team, *R: A Language and Environment for Statistical Computing*, R Foundation for Statistical Computing, Vienna, Austria, 2017. [Online]. Available: https://www.R-project.org/

[18] E. A. Peña and E. H. Slate, "Global validation of linear model assumptions," *Journal of the American Statistical Association*, vol. 101, no. 473, pp. 341–354, 2006.

[19] T. D. Fletcher, *psychometric: Applied Psychometric Theory*, 2010, r package version 2.2. [Online]. Available: https://CRAN.R-project.org/package=psychometric

[20] R. D. Morey and J. N. Rouder, *BayesFactor: Computation of Bayes Factors for Common Designs*, 2015, r package version 0.9.12-2. [Online]. Available: https://CRAN.R-project.org/package=BayesFactor

[21] B. B. McShane, D. Gal, A. Gelman, C. Robert, and J. L. Tackett, "Abandon statistical significance," *arXiv preprint arXiv:1709.07588*, 2017.

[22] R. L. Lieber, C. G. Brown, and C. L. Trestik, "Model of muscle-tendon interaction during frog semitendinosis fixed-end contractions," *Journal of biomechanics*, vol. 25, no. 4, pp. 421–428, 1992.

[23] S. F. Eby, P. Song, S. Chen, Q. Chen, J. F. Greenleaf, and K.-N. An, "Validation of shear wave elastography in skeletal muscle," *Journal of biomechanics*, vol. 46, no. 14, pp. 2381–2387, 2013.

[24] X. Hu, W. M. Murray, and E. J. Perreault, "Muscle short-range stiffness can be used to estimate the endpoint stiffness of the human arm," *Journal of neurophysiology*, vol. 105, no. 4, pp. 1633–1641, 2011.

[25] G. G. Handsfield, C. H. Meyer, J. M. Hart, M. F. Abel, and S. S. Blemker, "Relationships of 35 lower limb muscles to height and body mass quantified using mri," *Journal of biomechanics*, vol. 47, no. 3, pp. 631–638, 2014.

[26] G. G. Handsfield, J. M. Inouye, L. C. Slane, D. G. Thelen, G. W. Miller, and S. S. Blemker, "A 3d model of the achilles tendon to determine the mechanisms underlying nonuniform tendon displacements," *Journal of biomechanics*, vol. 51, pp. 17–25, 2017.